ROYAL SOCIETY OPEN SCIENCE

rsos.royalsocietypublishing.org

Research

Article submitted to journal

Subject Areas:
Engineering, Chemistry

Keywords:
polymer derived ceramic, fibers, CMC, ceramics, polymers

Author for correspondence:
Gurpreet Singh
e-mail: gurpreet@ksu.edu

Preparation and Structure of SiOCN Fibers Derived from Cyclic Silazane/PAA Hybrid Precursor

Zhongkan Ren[1], Christel Gervais[2] and Gurpreet Singh[1]

[1]Departement of Mechanical and Nuclear Engineering, Kansas State University, Manhattan, KS, 66506, USA
[2]Sorbonne Université, CNRS UMR 7574, Collège de France, Laboratoire de Chimie de la Matière Condensée de Paris, 75005 Paris, France

Ceramic matrix composite (CMC) materials have been considered a desired solution for lightweight and high temperature applications. Simultaneously, among all different CMC reinforcements, Polymer-Derived Ceramic (PDC) fibers have gained attention for the intrinsic thermal stability and mechanical strength with simple and cost-effective synthesis techniques. Here, carbon-rich SiOCN fibers were synthesized via hand-drawing and polymer pyrolysis of a hybrid precursor of 1,3,5,7-tetramethyl-1,3,5,7-tetravinyl-cyclotetrasilazane (TTCSZ) and polyacrylic acid (PAA). The type of silazane reported in this work is considered as a major precursor for SiCN fibers, although it is unspinnable if used pure, due to its unfavorable physical properties (low viscosity) and chemical structure (cyclic rather than linear structure). The introduction of PAA to TTCSZ to create a hybrid precursor remarkably improved spinnability of the silazane and should be widely applicable to other unspinnable PDC preceramic polymers. Investigations on structural and compositional development of the fibers were mainly conducted via Raman spectroscopy, Fourier-Transform InfraRed spectroscopy (FTIR), Scanning Electron Microscopy (SEM), X-ray Photoelectron Spectroscopy (XPS), Nuclear Magnetic Resonance (NMR) and ThermoGravimetric Analysis (TGA) to determine spinnability, free carbon content, cross-linking and pyrolysis behavior of the fibers,respectively.

THE ROYAL SOCIETY PUBLISHING

1. Introduction

Over the past few decades, there has been a rising desire for new structural aerospace materials with light-weight, high modulus and high thermal stability that has motivated the advance of materials science. Non-oxide ceramic matrix composites (CMCs) are known to fulfill all the demands because of the low density, remarkable mechanical strength and chemical resistance as well as elevated fracture toughness by fiber-reinforcement. The microporous and micro-cracked matrix allows several times higher strain-to-failure than monolithic ceramics that makes it one of the optimum structural materials at high temperature [1], while reinforcement contribution is mainly toward properties such as electrical conductivity, hardness, thermal expansion and shock resistance.

Polymer-Derived Ceramic Fibers (PDCFs) are considered an admirable reinforcement for CMCs due to improved properties and ease of fabrication by the recent innovations in polymer fiber fabrication technique [2]. Over last three decades, Si-based advanced ceramics with a variety of desirable properties, such as remarkable electrochemical behavior, chemical resistance, thermal stability and mechanical strength, have been designed with the help of straightforward polymer-to-ceramic conversion [3,4]. The mechanical properties of PDCFs have been reported as high as $2.5\,\mathrm{GPa}$ in tensile strength with $300\,\mathrm{GPa}$ in modulus while stay stable up to $2200\,^{\circ}\mathrm{C}$ [5].

With the rising demand for better processability, higher ceramic yield and enhanced properties of final ceramic product, numbers of new silicon based preceramic polymers were synthesized in the 1980s with modified properties that is sufficient enough for spinning [6–9]. The large-scale production of ceramic fibers started early as 1990s [10]. Either melt- or dry-spinning was applied to mainly polysilanes or polyborosilazanes to produce non-oxide SiC or SiBCN fibers. In terms of melt-spinning, modified polymer with required viscosity is continuously fed through a heated (about $150\,^{\circ}\mathrm{C}$) nozzle with hundreds of holes. Fibers are effectively drawn in this way and cured by additional thermal or chemical treatments [10]. Up until recently, there are many types of ceramic fibers developed over 20 years ago and still commercially available from various manufacturers, such as Hi-Nicalon (from COI), Sylramic (from UBE), etc.

Currently, both oxide or non-oxide (from polymer pyrolysis route) ceramic fibers are widely applied for high temperature applications. Oxide fibers usually delivers higher oxidation resistance compared to non-oxide fibers, while better creep resistance and strength retention allow non-oxide fibers to be even more suitable for ultrahigh temperature applications, such as aerospace components. However, polycarbosilane, main precursor of SiC fibers, is still costly and limited in availability. Hence, ceramic fibers with extremely lower cost and slightly compromised properties are of great interest [11–13]. On the contrary, other Si-based ceramics by PDC routes, such as SiCN ternary system was previously reported with as high oxidation resistance as $1300\,^{\circ}\mathrm{C}$ via cost-effective synthesis method [14]. The formation of SiO_2 and Si_2N_2O double layered structure generates increased diffusion barrier, thus to enhanced oxidation resistance [15,16]. Consequently, PDC precursors with higher N content should yield to elevated thermal and oxidation stability of the final ceramic products.

In this work, we report a new approach to synthesize carbon-rich SiOCN ceramic fibers via hand drawing and pyrolysis of a cyclic-silazane/PAA hybrid polymer. The hybrid approach involving hand spinning process is highly efficient for lab scale testing and to develop fundamental understanding related to processing of preceramic fibers and related polymer to ceramic transformations without the need for complex fiber drawing equipment. 1,3,5,7-tetramethyl-1,3,5,7-tetravinyl-cyclotetrasilazane (referred as TTCSZ in this article) is an organosilazane, whose properties have not been widely determined compared to the 1,3,5,7-tetramethyl-1,3,5,7-tetravinyl-cyclotetrasiloxane with similar molecular structure. This specific type of silazane is crosslinkable at elevated temperature, but not likely to directly draw fibers from. Hence, polyacrylic acid (PAA) is introduced to improve the fabrication or spinnability of pre-ceramic polymer fibers. As-prepared fibers were firstly crosslinked at lower temperature in open air, then pyrolyzed at higher temperature for polymer-to-ceramic conversion under the

protection of argon. Synthesis, characterization, pyrolysis manner and phase formation will be discussed in detail for TTCSZ/PAA hybrid fibers in the following sections.

2. Experimental

(a) Materials

All the syntheses were conducted with as-received materials without further treatment or purification. The TTCSZ is available from Gelest (USA). The polyacrylic acid (PAA) is purchased from Sigma-Aldrich (USA). Dicumyl peroxide (DCP) as crosslinking initiator is obtained from Sigma-Aldrich (USA). The fiber drawing, handling and crosslinking processes are performed in open air, except pyrolysis which is carried out in ultrahigh purity argon atmosphere from Matheson (USA).

(b) Fiber drawing and pyrolysis

TTCSZ/PAA hybrid fibers were prepared v ia sol-gel process (Fig. 1). 10 wt % of DCP initially dissolved in TTCSZ formed a solution. PAA was initially mixed with deionized water (PAA to di-water wt ratio 4:1) and stirred until the mixture turned completely into transparent gel. TTCSZ solution was then added to the gel (TTCSZ solution to PAA wt ratio 1:1). After complete mixing by stirring, the PAA/TTCSZ/water system formed a piece of white slurry with a viscosity measured to be about 250 P (Poise) or 25 Pa·s. The overall ratio between TTCSZ: DCP: PAA was 45: 5: 50 wt %. The fiber drawing process is carried out by hand drawing in open air. The hybrid fibers can be conveniently drawn directly from the slurry using metal rods, spatulas or tweezers onto aluminum boats for crosslinking process. Then the fibers are dried and crosslinked in a low temperature oven at 160 $^{\circ}$C for 24 hours in air. The aluminum boats are simply hand crafted with aluminum foils which have several advantages to be applied in this process. The aluminum foil is chemically and mechanically stable as a supporter that does not introduce extra impurities in low temperature open-air environment; the shrinkage of the hybrid fibers during crosslinking process can be well controlled by the boat; the scale of the boat can be determined by the size of the oven. Fibers are collected from aluminum boat after crosslinking, then relocated and wrapped on a small boat or rod support made with ceramics or quartz for high temperature pyrolysis.

The polymer-to-ceramic transformation is performed at three different temperatures (600, 700 and 900 $^{\circ}$C). The fibers on support are mounted on another alumina boat and heated from room temperature to target temperature at heating rate of 2 $^{\circ}$C/min under argon.

(c) Characterization

Surface morphology of the fibers at each stage was investigated by scanning electron microscopy (EVO MA10, ZEISS, Germany).

Raman spectroscopy was collected from LabRAM ARAMIS Raman spectrometer (LabRAM HORIBA Jobin Yvon, USA) using a HeNe laser (633 nm) as an excitation source.

Fourier-transform infrared spectroscopy (FT-IR) spectra was obtained from Spectrum 400 FT-IR spectrometer (Perkin Elmer, Waltham, MA) on a diamond crystal top plate of an ATR accessory (GladiATR, Pike Technologies, USA).

Viscosity measurement was performed on Brookfield DV-II+Pro viscometer (Brookfield Engineering, USA) using CEP-40 and CEP-52 cone for pure TTCSZ and TTCSZ/PAA, respectively. 0.5 mL slurry was used with 25 - 200 rpm rotation rate at 37 $^{\circ}$C for the measurement.

X-ray photoelectron spectroscopy (XPS) was performed by PHI Quantera SXM (ULVAC-PHI, Japan). Depth-profiling was applied for 15 mins via Ar ion-beam.

Solid-state ^{13}C MAS, CP MAS, and ^{29}Si MAS NMR spectra were recorded on a Bruker AVANCE 300 spectrometer (B_0 = 7.0 T, $\nu_0(^1H)$ = 300.29 MHz, $\nu_0(^{13}C)$ = 75.51 MHz, MHz, $\nu_0(^{29}Si)$ = 59.66 MHz) using either 4 mm or 7 mm Bruker probes and spinning frequencies of 10 or 5

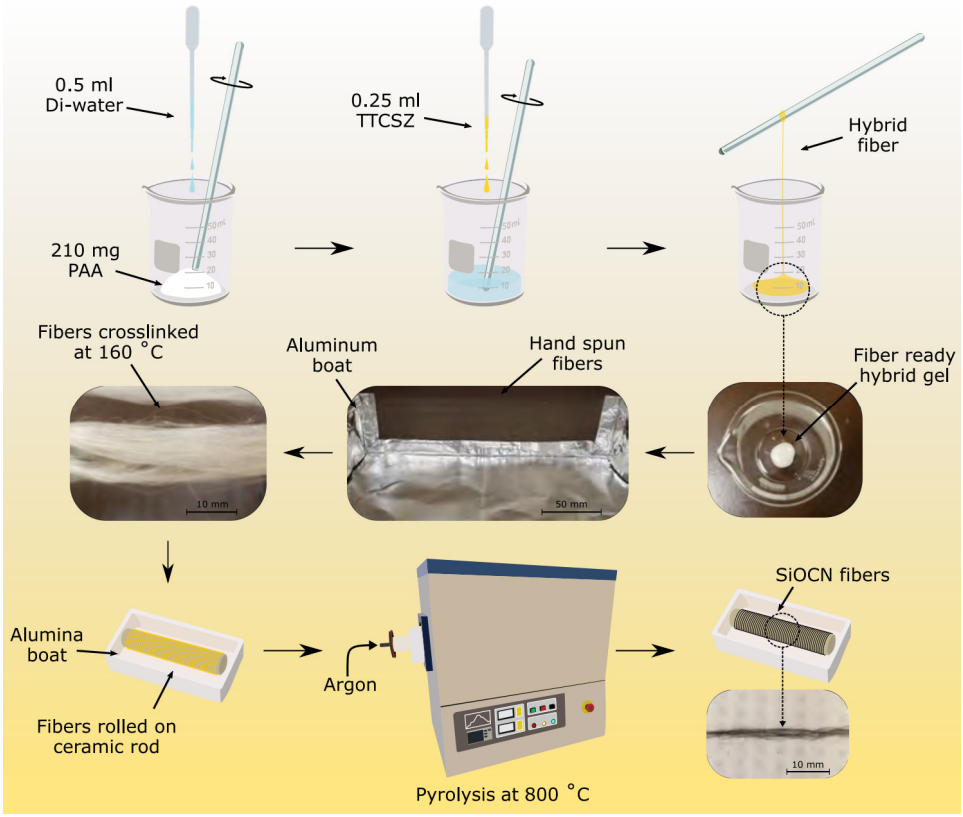

Figure 1. Schematics of fiber drawing process.

kHz. ^{13}C CP MAS experiments were recorded with ramped-amplitude cross-polarization in the ^{1}H channel to transfer magnetization from ^{1}H to ^{13}C. (Recycle delay = 3 s, CP contact time = 1 ms, optimized ^{1}H spinal-64 decoupling). Single pulse ^{13}C and ^{29}Si NMR MAS spectra were recorded with recycle delays of 30 and 60 s respectively. Chemical shift values were referenced to tetramethylsilane for ^{13}C and ^{29}Si.

The fiber thermal resistance was analyzed using thermal gravimetric analysis (TGA). The analysis was performed with TG 209 F1 Libra (NETZSCH, Germany) from 100 to 1000 °C (with heating rate of 10 °C min^{-1}) in either N_2 or synthetic air (with flow of 10 mL min^{-1}) for crosslinked, pyrolyzed TTCSZ/PAA and pure PAA samples.

3. Results and discussion

(a) Characterization of the hybrid fibers

A series of characterization was carried out to determine the properties of as pyrolyzed hybrid PDC fibers. SEM images of the pyrolyzed hybrid fibers are given in Fig. 3 a-c. It is confirmed by SEM that hand-spun fibers have a diameter range of $1 \sim 10$ µm. Each pyrolyzed fibers are considerably uniform in diameter and porous at the surface.

The chemical composition of PDC hybrid fibers are determined by XPS depth-profiling survey scans and the results are listed in Table 1. The presence of oxygen and loss of nitrogen are discussed in the following sections. The existence of "free carbon" was confirmed by

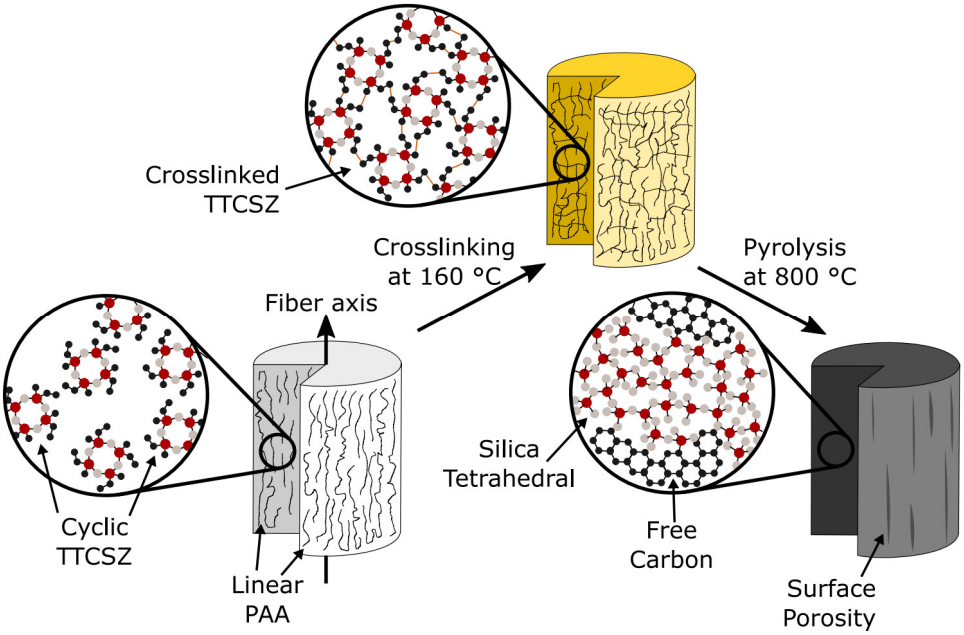

Figure 2. Schematics of fiber crosslinking and pyrolysis process. TTCSZ is the main PDC fiber precursor where PAA plays a fiber template role in the hybrid system. TTCSZ molecules are embedded in PAA rigid environment that can be crosslinked at elevated temperature. Within the fibers, PDC nano-domain structures are formed after pyrolyzed at even higher temperature.

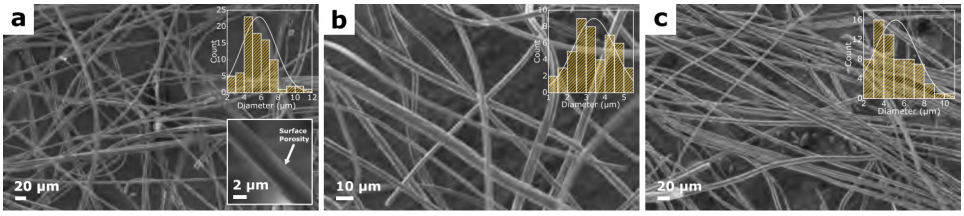

Figure 3. SEM images of hand spun TTCSZ/PAA hybrid fibers pyrolyzed at a) 600 $^{\circ}\mathrm{C}$, b) 700 $^{\circ}\mathrm{C}$ and c) 800 $^{\circ}\mathrm{C}$.Fibers have diameter distribution of 1 $\sim$ 10 $\mu\mathrm{m}$ with an average diameter about 5 $\mu\mathrm{m}$. When magnified, fiber surface porosity is noticeable.

Table 1. Chemical composition of fibers by XPS depth-profiling survey scan in atomic percentage

Pyrolysis	Element atomic percentage (at. %)			
Temperature (°C)	C	Si	O	N
700	71.2	8.6	19.4	0.3
800	50.8	15.5	33.4	0.4

Raman spectroscopy. Carbon G-band ($\sim$1595 cm^{-1}) (Fig. 4 d-e) shows the existence of graphitic sp^2 carbon structure in the fibers, while D-band ($\sim$1340 cm^{-1}) represents a large amount of disordered carbon [17]. Specifically, D4- and D3-bands indicate the existence of sp^2-sp^3 bonds and amorphous carbon in the fibers [17,18]. Carbon peaks are relatively weaker (high fluorescence) for

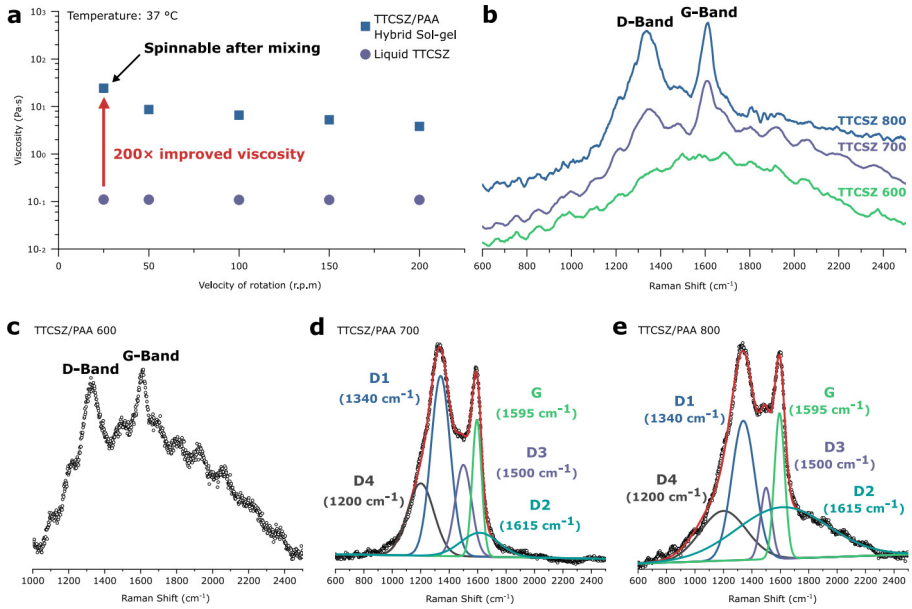

Figure 4. a) Viscosity of TTCSZ/PAA slurry and liquid TTCSZ. 200 times improved viscosity is observed after mixing with PAA which enhanced spinnability. b) Raman spectroscopy of pure TTCSZ pyrolyzed at different temperatures. TTCSZ/PAA hybrid fibers pyrolyzed at c) 600 °C, d) 700 °C and e) 800 °C. Free carbon amount is increased as raised pyrolysis temperature.

the fibers pyrolyzed at 600 °C indicating less free carbon. For the higher pyrolysis temperature, free carbon amount is significantly increased. Correspondingly, graphitic carbon is increased with the increase of pyrolysis temperature, while the amount of amorphous carbon is decreased. Because Si-C bonds are sp^3, stronger D1, D4-bands in 700 sample confirms higher SiO_2C_2 and SiO_3C composition discussed below with the NMR analysis (Fig. 5a) [19]. Raman spectra of pure TTCSZ samples are also obtained to find out the contribution of PAA to the pyrolyzed fibers (Fig. 4 b). The free carbon amounts are apparently raised with incorporation of PAA at initial stage by comparing the intensity of the carbon peaks. Further analysis was performed on bonding types and molecular structures. NMR spectroscopy investigation was performed on the samples at each pyrolysis temperature (Fig. 5). ^{29}Si MAS NMR spectrum (Fig. 5 a) of the sample heat-treated at 600°C shows components at $\sim$ −20 ppm, $\sim$ −65 ppm and $\sim$ −110 ppm suggesting tetrahedrally coordinated Si in SiO_2C_2, SiO_3C and SiO_4 species typical of mixed silicon oxycarbide units [20,21]. It should be noticed that part of the signal at $\sim$ −10 ppm could also correspond to SiN_2C_2 environments [22] but probably in small proportions. This point will be further discussed in part 3.3. The strong intensity of SiO_3C signal indicates a significant amount of C bonded to Si atoms and correspondingly less free carbon, this result well matches with the Raman data. When increasing the pyrolysis temperatures, the fractions of mixed silicon oxycarbide units decreases: SiO_3C peak greatly decreases and SiO_2C_2 peak disappears completely. SiO_3C peak further decreases at 800 °C and leaving most of Si atoms in silica tetrahedral form.

^{13}C CP MAS NMR results (Fig. 5 b) show a clear free carbon peak around 130 ppm for both 600 and 700 °C. No remaining vinyl groups are observed after pyrolysis suggesting a complete polymerization into aliphatic carbons while a strong Si-C peak is detected at 600 °C which drastically decreases at 700 °C.

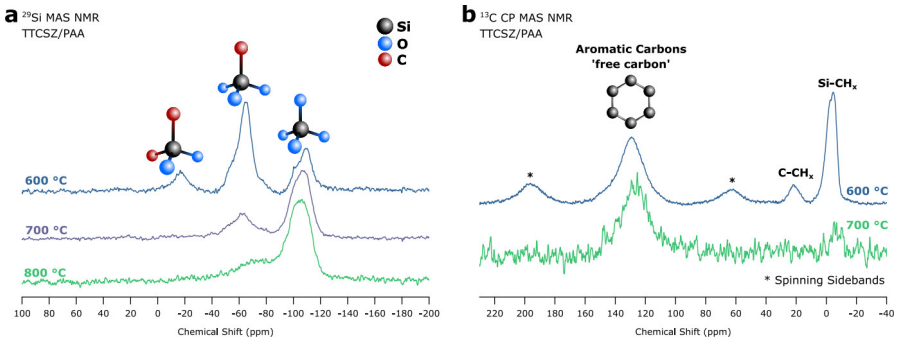

Figure 5. Solid-state NMR spectra of pyrolyzed TTCSZ/PAA hybrid fibers at 600, 700 and 800 °C (a) ^{29}Si MAS (b) ^{13}C CP MAS with corresponding micro structure shown. A significant drop in Si-C bonds is noticed as increasing of pyrolysis temperature. Number of scans (NS): ^{29}Si MAS 600 °C (NS = 1334), 700 °C (NS = 1122), 800 °C (NS = 4186); ^{13}C CP MAS 600 °C (NS = 2400), 700 °C (NS = 2784).

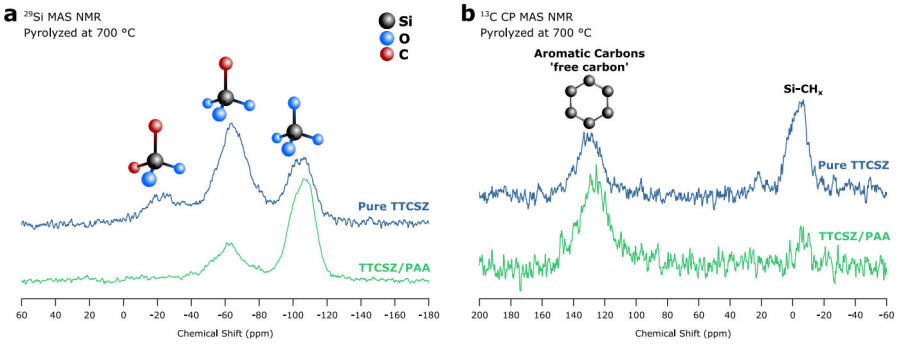

Figure 6. Solid-state NMR spectra of TTCSZ/PAA fibers and pure TTCSZ at 700 °C (a) ^{29}Si MAS (b) ^{13}C CP MAS. Under the same pyrolysis temperature, incorporation of PAA leads to increased free carbon and decreased Si-C bonds. Number of scans (NS): ^{29}Si MAS pure TTCSZ (NS = 1396), TTCSZ/PAA (NS = 1122); ^{13}C CP MAS pure TTCSZ (NS = 2736), TTCSZ/PAA (NS = 2784).

Further NMR spectra were recorded from TTCSZ/PAA hybrid fibers and pure TTCSZ powders samples pyrolyzed at 700 °C (Fig. 6) to investigate the effect of PAA on the structure of the final product. From the comparison, pure TTCSZ at 700 °C shows a spectrum very close to TTCSZ/PAA at 600 °C. As it has been already shown in Raman analysis, either incorporation of PAA or rising in pyrolysis temperature will ultimately result in a structure with elevated "free carbon" content and decreased Si-C bonds. This is also confirmed by ^{13}C CP MAS NMR data showing increased "free carbon" content and decreased Si-CH_x signals in TTCSZ/PAA hybrid sample compared to pure TTCSZ.

XPS analysis was applied to determine the bonding type (Fig. 7) from survey scan and high-resolution scan of O1s, C1s, Si2s, Si2p and N1s peaks in each samples [23]. From the survey scan, N1s peak disappears after pyrolysis above 600 °C. High resolution scans of major peaks reveals the merging of different signals, such as Si-C peaks at ∼102.0 eV in Si2p scan and ∼284.6 eV in C1s scan [23]. SiO_2C_2, SiO_3C and SiO_4 components can be obtained from hybrid fibers pyrolyzed at 600 °C in agreement with the NMR results [24]. From high-resolution C1s scan (Fig. 7 a.3, b.3,

c.3), the C-Si component is continuously decreased leading to relative increase in C-C as pyrolysis temperature increases. This result also matches the FT-IR spectra in Fig 8.

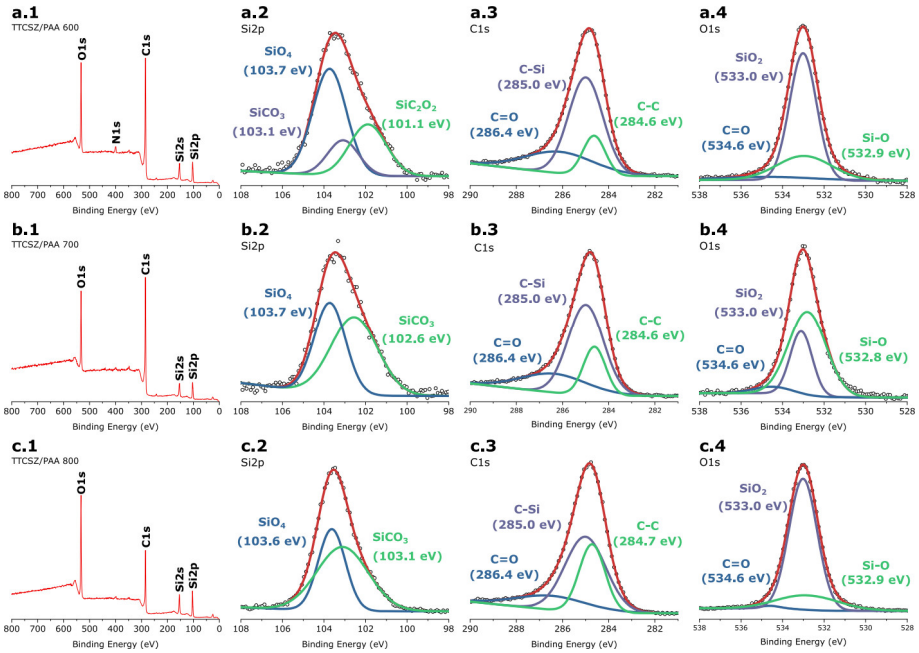

Figure 7. XPS results of PDC fibers from TTCSZ/PAA hybrid precursor. a-c.1) Survey scan. High resolution scan of Si2p, C1s and O1s of samples pyrolyzed at a.2-4) 600 °C, b.2-4) 700 °C and c.2-4) 800 °C. From a.3 to c.3, there is a huge increase in C-C/C-Si ratio.

(b) Spinnability

Initial attempts were made to draw fibers directly from pure liquid TTCSZ. The rapid crosslinking was observed at about 125 °C with 10 wt % crosslinking initiator DCP and completely transformed TTCSZ liquid into a hard bulk, without an intermediate viscous status that can initiate spinning process. The failure was due to two main reason: low viscosity (Fig. 4 a) and cyclic structure of TTCSZ. PAA was introduced to the initial fiber drawing stage before crosslinking to improve spinnability of TTCSZ. Viscosity measurement showed low viscosity (∼0.1 Pa·s at 37 °C) for liquid TTCSZ with 10 wt% DCP. After mixing with PAA, viscosity was raised more than 200 times to about 25 Pa·s at shear rate of 25 rpm (or 50 $\mathrm{cm\,s^{-1}}$) which met the requirement for sol-gel spinning (> 10 P) [25]. Besides, ^{13}C CP MAS NMR (Fig. 9) shows broad signals (suggesting low mobility) of $-CH(COOH)-CH_2-$ species which is responsible for enhanced spinnability.

(c) Crosslinking and pyrolysis behavior

Investigation of crosslinking behavior is essential since the final content of PDC fibers is largely determined by the bonds formed during crosslinking stage. FT-IR analysis were obtained with main bands characteristics of raw PAA fibers [26–28], pure PAA fibers heated at 160 °C, and TTCSZ/PAA hybrid raw, crosslinked and pyrolyzed fibers [29,30]. The weak influence of DCP on FT-IR signal is discussed in supplemental material (Fig. S1). FT-IR is mainly used to investigate

the crosslinking behavior of the precursors [29]. The changes between the precursor spectra and the crosslinked spectra reveal a critical loss of hydrogen and nitrogen during crosslinking. The excessive oxygen content is possibly imported by the initiator, adsorbed from the air or introduced during reaction with water (discussed below). Moreover, the majority of organic moieties (methyl and vinyl groups) are eliminated during this process along with the crosslinking evidence shown in the Fig. 8 a.

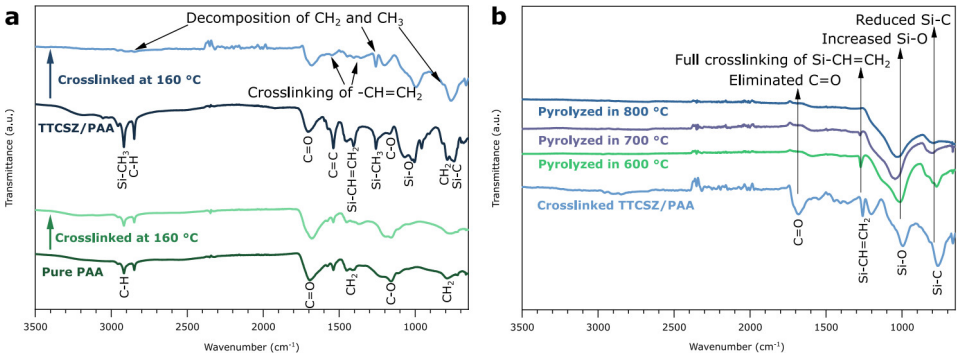

Figure 8. FT-IR spectra of TTCSZ/PAA hybrid fibers a) crosslinked at 130 °C, b) pyrolyzed at 600, 700 and 800 °C. At crosslinking stage, decomposition of CH_2 and CH_3, crosslinking of -CH=CH_2 are clearly observed.

NMR on raw and crosslinked samples supports FT-IR results in Fig. 9. Both ^{13}C MAS and ^{13}C CP MAS NMR were obtained for raw fibers to determine, respectively, highly mobile components (TTCSZ) and rigid environments (PAA). Before crosslinking, both ^{29}Si and ^{13}C MAS spectra show narrow signals indicating high mobility species: ^{29}Si peaks are mainly observed around –35 ppm, a position significantly different from the initial TTCSZ+DCP solution showing signals at –14.7 ppm and –17.5 ppm (Fig. 9a inset) characteristic of 6-ring 2,4,6-trimethyl-2,4,6-trivinylcyclotrisilazane [31] and 8-rings silazane TTCSZ respectively. Signals around –33 ppm are indeed reported for 1,3,5,7-tetravinyl-1,3,5,7-tetracyclotetrasiloxane [32]. This strongly suggests a significant oxidation of the silazane rings into siloxanes, possibly due to the addition of water with PAA. Nonetheless, additional minor signals are still present around –17 ppm, indicating that silazane bonds are still present.

At this point, from the strong evidence obtained from NMR analysis, two different hypotheses are proposed here to explain the loss of nitrogen before pyrolysis: (1) A large amount of the nitrogen loss may be addressed to the pre-spinning mixing stage. -NH- may react with H_2O molecules and form NH_3 inducing nitrogen loss before crosslinking.

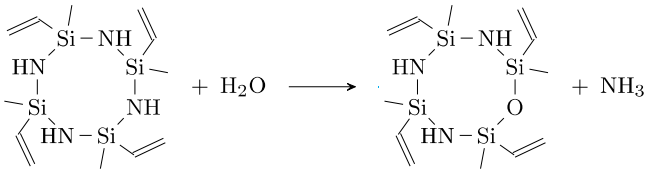

(2) During crosslinking stage, the hydrosilylation reaction takes place. This reaction is induced by heating and happens at relative lower temperature as low as 120 °C [33,34].

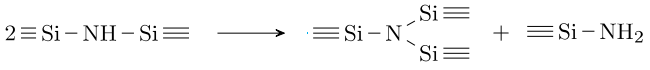

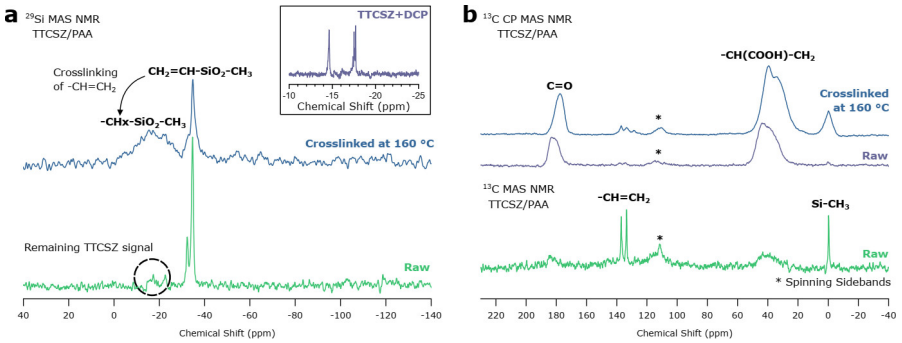

Figure 9. Solid-state NMR spectra of TTCSZ/PAA hybrid raw fibers and crosslinked fibers. ^{29}Si MAS NMR result indicates decreased mobility after crosslinking, and ^{13}C showed very low interaction between PAA (rigid environment) and TTCSZ at crosslinking stage. Number of scans (NS): ^{29}Si MAS Crosslinked at 160 °C (NS = 474), Raw (NS = 140); ^{13}C CP MAS Crosslinked at 160 °C (NS = 1056), Raw (NS = 432); ^{13}C MAS Raw (NS = 56).

$$\equiv Si-NH_2 \;+\; \equiv Si-NH-Si\equiv \;\longrightarrow\; \equiv Si-N\begin{matrix}Si\equiv\\ Si\equiv\end{matrix} \;+\; NH_3$$

As a result, TTCSZ may be oxidized to 1, 3, 5, 7-tetramethyl-1, 3, 5, 7-tetravinyl-cyclotetrasiloxane. Then methyl-vinyl radical reaction will take place initiated by DCP during crosslinking stage. The reaction can be shown as follow [35].

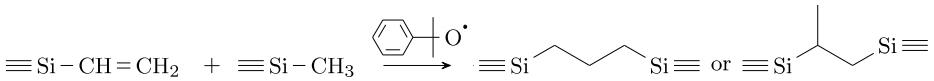

And the reactions are expected to take place on all four vinyl groups attached to four cyclic silicon atoms and form into network structure. However, this crosslinking reaction may not be complete due to the limited mobility after the network formation [34,35].

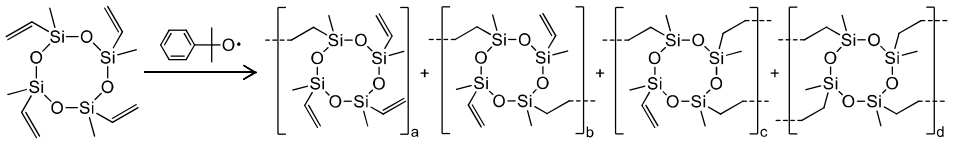

After crosslinking at 160 °C, broader peaks indicate less mobility due to the conversion of Vi−(Me)SiO$_2$ to −CH$_2$−(Me)SiO$_2$. However, high consistency between raw and 160 °C ^{13}C CP MAS suggests very weak PAA crosslinking activities at 160 °C. Further discussion regarding crosslinking behavior between PAA and TTCSZ is presented in supplemental material (Fig. S2).

Polymer-to-ceramic conversion process is revealed at 600 °C which is supported by Raman analysis showing free carbon bands in Fig. 3. However, Comparison of FTIR results between crosslinked fibers and pyrolyzed fibers suggests that the conversion is not complete until 800 °C. The decomposition of remaining organic groups is observed at pyrolysis temperature range (600 - 800 °C).

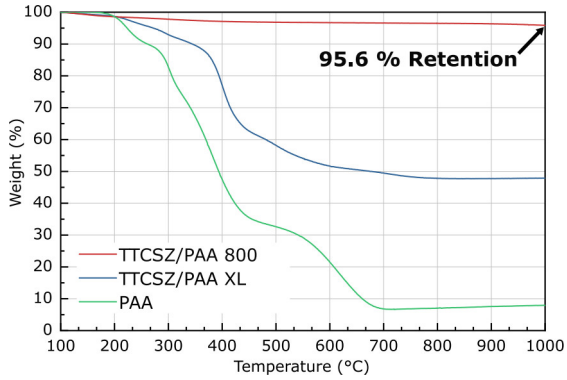

Figure 10. TGA analysis of TTCSZ/PAA hybrid pyrolyzed at 800 °C and weight change recorded in N_2; TTCSZ/PAA hybrid crosslinked at 160 °C and weight change recorded in N_2; pure PAA sample and weight change recorded in air.

(d) Thermal resistance

The thermal behavior of the hybrid fibers is studied with thermogravimetric analysis using powder samples in either N_2 or air and the results are shown in (Fig. 10). The significant weight loss of pure PAA fibers started at a temperature as low as 200 °C. The hybrid fibers pyrolyzed at 800 °C showed a good thermal stability up to 1000 °C with weight loss of 4.5 wt. %. While the TGA curve of crosslinked hybrid samples gives a rough idea of ceramic yield of this TTCSZ/PAA combination. The estimated yield in of crosslinked sample is about 48 % according to (Fig. 10) which well matches with the recorded ceramic yield. TGA result of pure PAA in air, associated with NMR results, indicates that PAA in the hybrid system mainly acts as a fiber template (rigid environment mentioned above) in the spinning process and does not participate in crosslinking (^{13}C CP MAS NMR), and provides a small amount of excessive carbon after pyrolysis.

4. Conclusion

Carbon-rich SiOCN fibers are synthesized and reported in this work, for the first time, from commercially available 1,3,5,7-tetramethyl-1,3,5,7-tetravinyl-cyclotetrasilazane and PAA forming a hybrid preceramic polymer precursor. The sol-gel process, fiber drawing and crosslinking processes are easily conducted in open air. Linear PAA molecules provide rigid body during fiber drawing process and provide excessive free carbon in the final fiber product. As-spun fibers are revealed oxygen rich which may be due to the presence of water during mixing stage, still, providing intrinsic thermal stability at 1000 °C.

The fibers products are uniform in diameter with a small degree of surface porosity (without large defects) observed during the characterization even with hand spinning. The spinning process and technique developed in this work successfully produced fibers from an unspinnable silazane with acceptable compromise in composition and properties, but greatly reduced processing cost and environmental requirement. This hybrid technique is recommended to lab scale early production of new types of ceramic fibers. High productivity of this technique can easily satisfy various characterization needs with minimum setup requirement.âĂİ The fiber products are suggested as reinforcement for CMC materials.

The fibers structure and properties may be improved by altering synthesis condition. Oxygen content can be controlled from the initial fiber drawing stage to crosslinking stage: instead of mixing TTCSZ/PAA in aqueous environment, melt-spinning is applicable to avoid the reaction between TTCSZ and water molecule, where this process can be conducted in a glovebox;

crosslinking environment can be adjusted to inert atmosphere such as N_2 or Ar to avoid fibers from direct contact with O_2; crosslinking method can also be altered to irradiation (gamma or electron), photo (UV) or ionic crosslinking instead of thermal crosslinking.

Data accessibility. Raw data are available within the Dryad Digital Repository [36]: https://doi.org/10.5061/dryad.bt45780

Authors' contributions. G.S. participated in design of the project as senior researcher and helped with drafting the manuscript; C.G. contributes to perform characterizations, data analysis and drafted the manuscript; Z.R. carried out preparation of all samples, data analyses and drafted the manuscript;

Competing interests. The authors declare no competing interests.

Funding. Financially support from National Science Foundation grant number 1743701 is gratefully acknowledged.

Acknowledgements. C. Gervais thanks F. Ribot for fruitful discussions. Thanks are also due to undergraduates MacKenzy Meis and Isabella Cesarone for help with material preparation. Special thanks to Dr. Qiang Ye from Institute for Bioengineering Research Laboratories, University of Kansas for equipment (Raman, FTIR and Viscometer) training and technical support.

References

1. Krenkel W. 2004 Carbon fiber reinforced CMC for high-performance structures. *International Journal of applied ceramic technology* **1**, 188–200. (doi:10.1111/j.1744-7402.2004.tb00169.x)
2. Bernard S, Weinmann M, Gerstel P, Miele P, Aldinger F. 2005 Boron-modified polysilazane as a novel single-source precursor for SiBCN ceramic fibers: synthesis, melt-spinning, curing and ceramic conversion. *Journal of materials chemistry* **15**, 289–299. (doi:10.1039/B408295H)
3. Laine RM, Babonneau F. 1993 Preceramic polymer routes to silicon carbide. *Chemistry of materials* **5**, 260–279. (doi:10.1021/cm00027a007)
4. Cinibulk MK, Parthasarathy TA. 2001 Characterization of oxidized polymer-derived SiBCN fibers. *Journal of the American Ceramic Society* **84**, 2197–2202. (doi:10.1111/j.1151-2916.2001.tb00987.x)
5. Ishikawa T, Kohtoku Y, Kumagawa K, Yamamura T, Nagasawa T. 1998 High-strength alkali-resistant sintered SiC fibre stable to 2,200 C. *Nature* **391**, 773. (doi:10.1038/35820)
6. King RE, Kanner B, Hopper SP, Schilling CL. *Method for making polysilazanes* US patent; 4675424. 1987 .
7. Serita T, Takeuchi H. *Method for making polysilazane* US patent; 4725660. 1988 .
8. Takeuchi H, Noake K, Serita T. *Polysilazane and method for synthesis thereof* US patent; 4950381. 1990 .
9. Ayama K, Noake K, Serita T. *New polysilazane and process for production of the same* US patent; 4937304. 1990 .
10. Baldus P, Jansen M, Sporn D. 1999 Ceramic fibers for matrix composites in high-temperature engine applications. *Science* **285**, 699–703. (doi:10.1126/science.285.5428.699)
11. Flores O, Bordia RK, Nestler D, Krenkel W, Motz G. 2014 Ceramic fibers based on SiC and SiCN systems: Current research, development, and commercial status. *Advanced Engineering Materials* **16**, 621–636. (doi:10.1002/adem.201400069)
12. Zok FW. 2016 Ceramic-matrix composites enable revolutionary gains in turbine engine efficiency. *Am Ceram Soc Bull* **95**, 22–8.
13. Naslain R. 2004 Design, preparation and properties of non-oxide CMCs for application in engines and nuclear reactors: an overview. *Composites Science and Technology* **64**, 155–170. (doi:10.1016/S0266-3538(03)00230-6)
14. Flores O, Bordia R, Bernard S, Uhlemann T, Krenkel W, Motz G. 2015 Processing and characterization of large diameter ceramic SiCN monofilaments from commercial oligosilazanes. *RSC Advances* **5**, 107001–107011. (doi:10.1039/C5RA17300K)
15. Chollon G. 2000 Oxidation behaviour of ceramic fibres from the Si–C–N–O system and related sub-systems. *Journal of the European Ceramic Society* **20**, 1959–1974.

(doi:10.1016/S0955-2219(00)00101-1)
16. Mocaer D, Pailler R, Naslain R, Richard C, Pillot J, Dunogues J, Gerardin C, Taulelle F. 1993 Si-CN ceramics with a high microstructural stability elaborated from the pyrolysis of new polycarbosilazane precursors. *Journal of materials science* **28**, 2615–2631. (doi:10.1007/BF00356196)
17. Mera G, Navrotsky A, Sen S, Kleebe HJ, Riedel R. 2013 Polymer-derived SiCN and SiOC ceramics–structure and energetics at the nanoscale. *Journal of Materials Chemistry A* **1**, 3826–3836. (doi:10.1039/C2TA00727D)
18. Bokobza L, Bruneel JL, Couzi M. 2014 Raman spectroscopy as a tool for the analysis of carbon-based materials (highly oriented pyrolitic graphite, multilayer graphene and multiwall carbon nanotubes) and of some of their elastomeric composites. *Vibrational Spectroscopy* **74**, 57–63. (doi:10.1016/j.vibspec.2014.07.009)
19. Saha A, Shah SR, Raj R. 2003 Amorphous silicon carbonitride fibers drawn from alkoxide modified cerasetÂŹ. *Journal of the American Ceramic Society* **86**, 1443–1445. (doi:10.1111/j.1151-2916.2003.tb03493.x)
20. Pantano CG, Singh AK, Zhang H. 1999 Silicon Oxycarbide Glasses. *Journal of Sol-Gel Science and Technology* **14**, 7–25. (doi:10.1023/A:1008765829012)
21. Sorarù GD, D'andrea G, Campostrini R, Babonneau F, Mariotto G. 1995 Structural characterization and high-temperature behavior of silicon oxycarbide glasses prepared from sol-gel precursors containing Si-H bonds. *Journal of the American Ceramic Society* **78**, 379–387. (doi:10.1111/j.1151-2916.1995.tb08811.x)
22. Gervais C, Babonneau F, Ruwisch L, Hauser R, Riedel R. 2003 Solid-state NMR investigations of the polymer route to SiBCN ceramics. *Canadian journal of chemistry* **81**, 1359–1369. (doi:10.1139/v03-167)
23. David L, Bhandavat R, Barrera U, Singh G. 2016 Silicon oxycarbide glass-graphene composite paper electrode for long-cycle lithium-ion batteries. *Nature communications* **7**, 10998. (doi:10.1038/ncomms10998)
24. Corriu R, Leclercq D, Mutin P, Vioux A. 1997 Preparation and structure of silicon oxycarbide glasses derived from polysiloxane precursors. *Journal of Sol-Gel Science and Technology* **8**, 327–330. (doi:doi.org/10.1007/BF02436860)
25. Su D, Yan X, Liu N, Li X, Ji H. 2016 Preparation and characterization of continuous SiZrOC fibers by polyvinyl pyrrolidone-assisted sol–gel process. *Journal of materials science* **51**, 1418–1427. (doi:10.1007/s10853-015-9461-7)
26. Kam W, Liew CW, Lim J, Ramesh S. 2014 Electrical, structural, and thermal studies of antimony trioxide-doped poly (acrylic acid)-based composite polymer electrolytes. *Ionics* **20**, 665–674. (doi:10.1007/s11581-013-1012-0)
27. Verma D, Katti K, Katti D. 2006 Experimental investigation of interfaces in hydroxyapatite/polyacrylic acid/polycaprolactone composites using photoacoustic FTIR spectroscopy. *Journal of Biomedical Materials Research Part A: An Official Journal of The Society for Biomaterials, The Japanese Society for Biomaterials, and The Australian Society for Biomaterials and the Korean Society for Biomaterials* **77**, 59–66. (doi:10.1002/jbm.a.30592)
28. Kirwan LJ, Fawell PD, van Bronswijk W. 2003 In situ FTIR-ATR examination of poly (acrylic acid) adsorbed onto hematite at low pH. *Langmuir* **19**, 5802–5807. (doi:10.1021/la027012d)
29. Li Q, Yin X, Duan W, Hao B, Kong L, Liu X. 2014 Dielectric and microwave absorption properties of polymer derived SiCN ceramics annealed in N2 atmosphere. *Journal of the European Ceramic Society* **34**, 589–598. (doi:10.1016/j.jeurceramsoc.2013.08.042)
30. Nyczyk A, Paluszkiewicz C, Pyda A, Hasik M. 2011 Preceramic polysiloxane networks obtained by hydrosilylation of 1, 3, 5, 7-tetravinyl-1, 3, 5, 7-tetramethylcyclotetrasiloxane. *Spectrochimica Acta Part A: Molecular and Biomolecular Spectroscopy* **79**, 801–808. (doi:10.1016/j.saa.2010.08.056)
31. Nghiem QD, Jeon JK, Hong LY, Kim DP. 2003 Polymer derived Si–C–B–N ceramics via hydroboration from borazine derivatives and trivinylcyclotrisilazane. *Journal of organometallic chemistry* **688**, 27–35. (doi:10.1016/j.jorganchem.2003.08.025)
32. Ziemelis MJ, Saam JC. 1989 Sequence distribution in

poly (dimethylsiloxane-co-methylvinylsiloxanes). *Macromolecules* **22**, 2111–2116. (doi:10.1021/ma00195a017)

33. DâĂŹElia R, Dusserre G, Del Confetto S, Eberling-Fux N, Descamps C, Cutard T. 2016 Cure kinetics of a polysilazane system: Experimental characterization and numerical modelling. *European Polymer Journal* **76**, 40–52. (doi:10.1016/j.eurpolymj.2016.01.025)
34. Schiavon MA, Soraru GD, Yoshida IVP. 2002 Synthesis of a polycyclic silazane network and its evolution to silicon carbonitride glass. *Journal of Non-Crystalline Solids* **304**, 76–83. (doi:10.1016/S0022-3093(02)01007-4)
35. Schmidt WR, Narsavage-Heald DM, Jones DM, Marchetti PS, Raker D, Maciel GE. 1999 Poly (borosilazane) precursors to ceramic nanocomposites. *Chemistry of materials* **11**, 1455–1464. (doi:10.1021/cm980558u)
36. Ren Z, Gervais C, Singh G. 2019 Data from: Preparation and Structure of SiOCN Fibers Derived from Cyclic Silazane/PAA Hybrid Precursor. Dryad Digital Repository. (doi:10.5061/dryad.bt45780)